The effect of slider texture on the tribology of near contact recording sliders

L. Zhou[a], M. Beck[b], H.H. Gatzen[b], K. Kato[c], G. Vurens[d], and F.E. Talke[a,*]

[a]*Center for Magnetic Recording Research, University of California, San Diego, USA*
[b]*Institute for Microtechnology, Hannover University, Hannover, Germany*
[c]*Laboratory of Tribology, School of Mechanical Engineering, Tohoku University, Sendai, Japan*
[d]*HDI Instrumentation, Santa Clara, USA*

Received 14 February 2003; accepted 22 September 2003

Island-type texture was fabricated on two types of pico-sliders using plasma etching and ion beam etching. Laser–Doppler interferometry was used to investigate the vibrations of textured and untextured pico-sliders in near-contact situations. Lubricant depletion on the disk surface was investigated in the slider "wear tracks" using scanning ellipsometry (Surface Reflectance Analyzer (SRA)). The results show that slider in-plane and out-of-plane vibrations were reduced as a consequence of the texture on the slider surface. In addition, lubricant depletion on the disk surface was found to be less severe for textured sliders than for untextured sliders at flying heights below 10 nm.

KEY WORDS: hard disk slider, texture, near contact recording, tribology

1. Introduction

To increase the recording density of hard disk drives, the flying height between slider and disk must be reduced. In order to achieve a recording density of 100 Gb/in^2, it has been suggested that the flying height of a slider would need to be about 6 to 7 nm [1]. Flying heights on the order of 6 to 7 nm require that the surface roughness of the disk must be very small. A very smooth disk surface is undesirable, however, since increased stiction between slider and disk can lead to failure of the head/disk interface.

To reduce stiction between slider and disk and achieve high recording density, "zone texturing" of disks has been implemented in recent years [2]. In this approach, the surface roughness of the start/stop region is increased to reduce stiction, while the surface roughness in the data zone is decreased to allow very low flying. When the disk drive is not in operation the slider "rests" on the surface roughness of the start/stop zone. A commonly used implementation of zone texturing is the so-called "laser texturing", where small craters in the start/stop zone are created by a high-power laser pulse [3,4].

To allow a further reduction of the flying height, the so-called load/unload technology was recently implemented [5,6]. In this approach, the slider is removed from the disk surface by means of a ramp before the disk comes to rest. For load/unload drives, so-called "super smooth disks" can be used featuring centerline surface roughness values of less than 0.25 nm. Since load/unload technology requires very tight tolerances of the ramp load mechanism, the question arises as to whether it would be possible to use a "super-smooth" disk without a load/unload mechanism. In this regard, "padded" sliders have been investigated [7,8] which have a number of cylindrical pads or micro-asperities on the air-bearing surface. The number and the size of the pads determine the real area of contact between slider and disk during start/stop and control the meniscus forces between the smooth disk and the slider. Padded sliders have been shown to reduce the stiction between slider and disk [7,8], and have been successfully implemented in commercial products.

An alternative to using padded sliders would be to use textured sliders, since textured sliders would also reduce the real contact area between slider and disk. In this way, textured sliders would control the stiction of the head/disk interface by limiting the formation of meniscus bridges at the head/disk interface. Similar to the padded slider approach, the texture on the slider will not contribute to the effective magnetic spacing as long as the pole tip region of the magnetic head is not recessed [9].

A number of research efforts on the effect of slider texture have been conducted in the past. The first to propose the use of textured sliders was Chen [10]. He used mechanical methods to roughen the slider surface. Zhou *et al.* [11,12] proposed a slider surface texturing method using ion beam etching. In their study, the friction between slider and disk was measured as a function of surface roughness in a constant speed drag

* To whom correspondence should be addressed.
E-mail: ftalke@ucsd.edu

1023-8883/04/0500–0297/0

test. The results showed that a critical value of peak to valley surface roughness exists, below which the friction is high and above which the friction is low. Interferometric lithography was recently implemented by Hanchi *et al.* to fabricate textured sliders [13]. Their results showed that texture on a slider surface was effective in reducing the friction between the slider and the disk in the near-contact regime. Ion beam textured sliders were also studied by Xu *et al.* to investigate the effect of slider surface texture on slider vibrations caused by contact [14]. They found that textured sliders were effective in reducing contact-induced vibrations of air-bearing modes. Recently, a study of textured nano-sliders by Zhou *et al.* [9] showed that textured sliders exhibited less lubricant displacement and slider vibrations than untextured sliders at a flying height of 7 nm. In [9], the flying height of 7 nm was achieved by reducing the disk rotational speed to the range of 1000 to 1500 rpm. Since a reduction in the disk velocity changes the stiffness of the air bearing and the dynamic behavior of the slider/disk interface, the question arises as to whether the beneficial effects of texture will still hold if the flying height of the head/disk interface is decreased to less than 7 nm by changing the air bearing design rather than by reducing the disk velocity.

Preliminary research using a 7 nm flying slider at 7200 rpm disk speed (15 m/s) showed promising results with respect to the effect of texture on friction [15]. To further study the tribological properties of textured sliders at even lower flying heights, and compare the slider dynamics of textured and untextured sliders at normal and reduced disk speeds, the research presented in this paper was performed. Two types of newly designed pico-sliders were textured using ion beam etching and argon plasma etching. The dynamics of these sliders was analyzed as a function of disk rotational speed and disk radius using Laser–Doppler Vibrometry (LDV). In addition, the effect of slider surface texture on lubricant depletion on the disk surface was studied using scanning ellipsometry (Surface Reflectance Analyzer (SRA)).

2. Experiments

2.1. Samples

Figure 1 shows the air-bearing surface designs of the two types of pico-sliders used. The design flying height for slider A is 15 nm at 4200 rpm while it is 7 nm at 7200 rpm for slider B. Two types of disks were used, a so-called "laser-textured disk" with laser bumps in the start/stop zone (disk A), and a so-called "super-smooth disk" without laser bumps (disk B). Disk A was coated with 5 nm of hydrogenated carbon and 1.8 nm of Z-Dol4000, while disk B was coated with 3 nm of nitrogenated carbon and 1.2 nm of PFPE lubricant. The average surface roughness (Ra) of the disks was

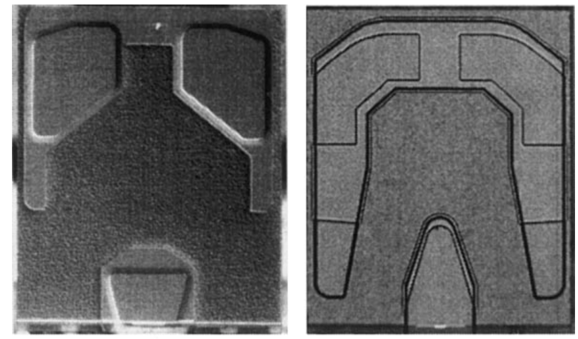

Figure 1. Slider air-bearing surface design.

0.35 nm and 0.24 nm (measured using AFM) for disk A and B, respectively.

2.2. Texturing of sliders

The most commonly used slider material for magnetic recording sliders is alumina titanium carbide, which is a hard ceramic consisting of two phases, i.e., Al_2O_3 and TiC. Al_2O_3 and TiC exhibit different etch rates when exposed to a beam of energized particles. This results in a change of the topography of the slider surface, i.e., the phase with the higher etching rate becomes recessed relative to the phase with the lower etching rate. Figure 2 shows a typical AFM image of a textured slider surface used in our work produced by ion beam etching. Similar results can be obtained using argon plasma etching. The texture height was controlled by adjusting the etching dose.

Slider A was textured using ion beam etching. Nitrogen ions of 1 keV were used at intensities of 1.13×10^{17} ion/cm^2, 1.50×10^{17} ion/cm^2 and 2.25×10^{17} ion/cm^2. After texturing, the TiC formed "islands" on the slider surface. The size of these "islands" corresponds to the grain size of the TiC, generally on the order of several micrometers. The island height achieved was 2, 3, and 4.7 nm, respectively, corresponding to the three etching doses used. In order to obtain good tribological performance of the textured sliders, a

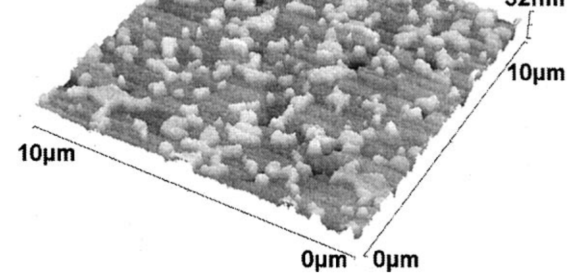

Figure 2. A typical AFM image of a textured slider surface.

7 nm wear resistant protective diamond like carbon coating was deposited on the textured sliders [16,17].

Slider B was etched using argon plasma with a power of 100 Watts at a pressure of 0.05 mbar. The texture height was controlled by adjusting the etching time. A texture height of 4.5 nm was achieved using 4 min etching, while 15 min etching resulted in a texture height of 9.5 nm. A wear resistant carbon overcoat of 8 nm was deposited on the textured and untextured sliders using plasma-enhanced chemical vapor deposition (PECVD).

2.3. Flying height and slider dynamics measurements

The flying height of sliders A before and after texturing as a function of velocity was measured using a commercially available flying height tester (DFHT). A Laser–Doppler Vibrometer (LDV) was used to observe the in-plane and out-of-plane vibration modes of the textured and the untextured slider A flying over disk A at a flying height of 15 and 4 nm, respectively. The 4 nm flying height of slider A was obtained by reducing the disk rotational speed to 1000 $\sim$ 1500 rpm (about 3 m/s). In order to investigate the dynamic characteristics at regular disk speed, the out-of-plane vibrations of textured and untextured slider B flying over disks A and B were also observed using Laser–Doppler Vibrometry at disk speeds of 5400 rpm and 7200 rpm, respectively.

For the measurement of slider in-plane vibrations, the LDV laser beam was focused horizontally on the side of the slider. A sampling rate of 100 kHz was used together with a band-pass filter from 1 to 50 kHz. The skew angle was set at 15 degrees to observe the suspension modes excited by friction force. For the measurement of slider out-of-plane vibrations, the laser beam was focused vertically near the inner trailing edge of the slider. The sampling rate used was 4 MHz, and the band-pass filter was set from 1 kHz to 1.5 MHz. The skew angle was set to 0 degrees.

2.4. Glide tests

The untextured and the 4.7 nm textured sliders of type A were tested on disk A at a flying height of 4 nm for 240,000 passes. The lubricant redistribution on the disk surface after the tests was analyzed using the Surface Reflectance Analyzer (SRA).

The untextured and the 4.5 nm textured sliders of type B were tested on disk B at the middle disk diameter. The disk speed was set at 7200 rpm (about 7 nm flying height). The tests at the middle diameter were stopped after 432,000 passes. The lubricant redistribution on the disk surfaces was analyzed using the Surface Reflectance Analyzer (SRA).

3. Experimental results

3.1. Flying height measurements of textured and untextured slider A

The flying height of textured and untextured slider A as a function of disk speed is shown in figure 3(a). Each data point represents an average of five measurements. The flying height differences before and after texturing as a function of texture height are shown in figure 3(b). The differences in the flying height before and after etching are in the range of ± 0.5 nm. These differences are smaller than the difference between individual untextured sliders of the same type for identical conditions. Thus, it appears that texturing does not affect the flying height of the sliders significantly, if the texture height is less than approximately 4.5 nm. However, if the texture height increases to values on the order of 10 nm, an increasing reduction in flying height is observed.

3.2. Slider dynamics

Figure 4 shows the frequency spectrum of the "in-plane" motion of slider A flying on disk A as a function of texture height. At a flying height of 15 nm (figure 4(a)), in-plane vibration modes are absent. On the other hand, at a flying height of 4 nm (figure 4(b)), suspension torsion modes at 5300 Hz and sway modes at 8500 Hz are clearly noticeable in the frequency spectrum. The

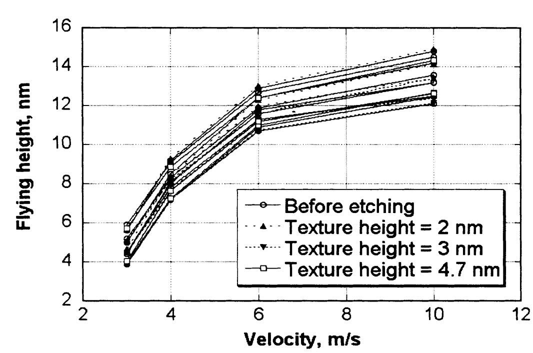

(a) Flying height vs. disk velocity

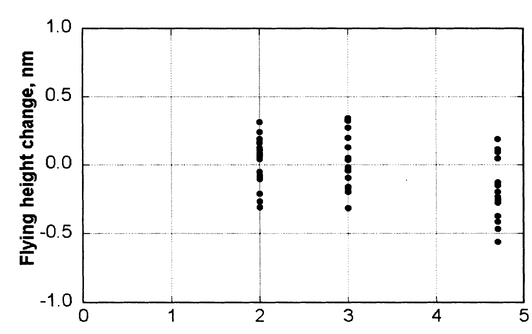

(b) Flying height changes vs. texture height

Figure 3. Flying height measurements for slider A before and after etching.

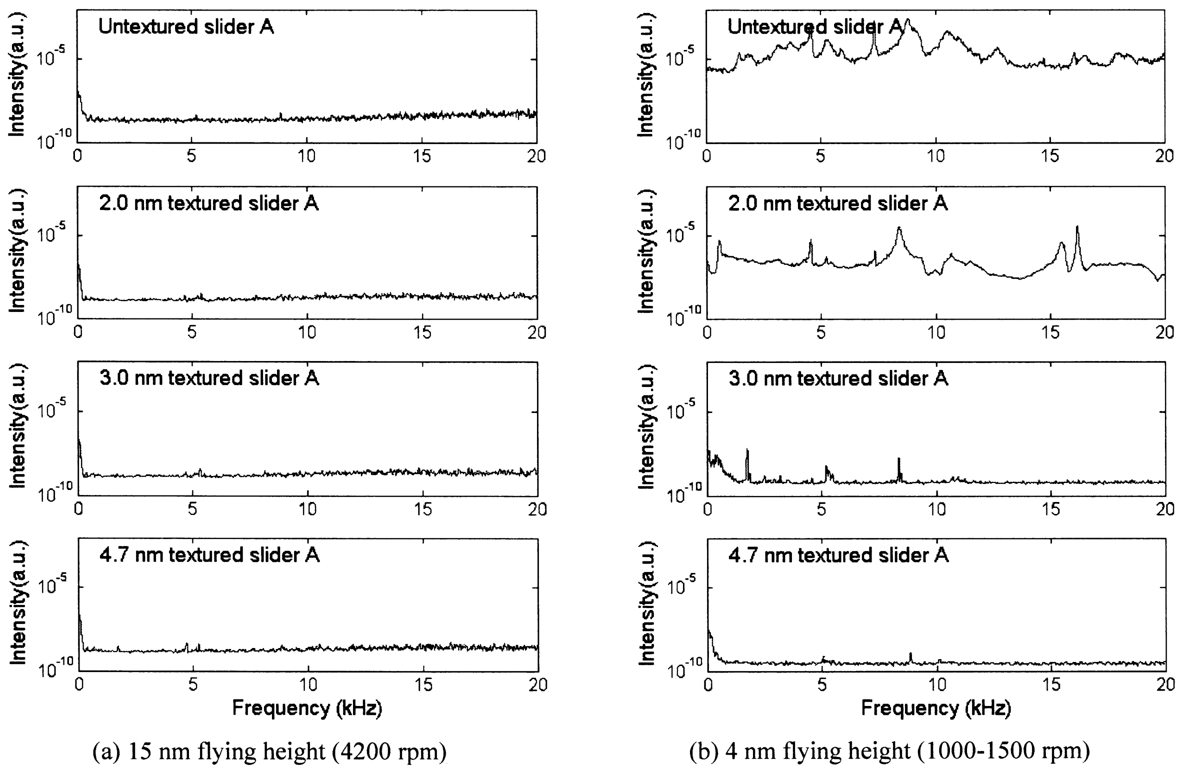

Figure 4. In-plane frequency spectrum of slider A as a function of texture height.

intensity of the two modes decreases with increasing texture height.

Figure 5 shows the frequency spectrum of the "out-of-plane" motion for untextured and 4.7 nm textured slider A flying on disk A. Air bearing modes (< 200 kHz) are observed at a flying height of 15 nm. The intensity of these air bearing modes increased dramatically at a flying height of 4 nm. For the untextured slider at a flying height of 4 nm, the first slider bending mode at 1.6 MHz is observed. This mode is absent for the 4.7 nm textured slider at the same flying height.

The out-of-plane vibration spectra of untextured and texture sliders B (4.5 and 9.5 nm texture height) flying on disk A at disk speeds of 5400 and 7200 rpm, respectively, are shown in figure 6. Air-bearing modes (< 200 kHz) are observed in all spectra, while slider-torsion modes at 1.3 MHz and bending modes at 1.6 MHz are observed only for the untextured and the 9.5 nm textured sliders at the inner diameter on disk A at 5400 rpm. Figure 7 shows the out-of-plane vibration spectra of slider B flying on disk B at 5400 and 7200 rpm, respectively. Slider torsion and bending modes are observed for the untextured and the 9.5 nm textured sliders at the inner diameter on disk B at both 5400 and 7200 rpm. The intensity of the two modes at 7200 rpm is lower than that at 5400 rpm. The two slider vibration modes are absent for the 4.5 nm textured sliders on disk A and B at both 5400 and 7200 rpm.

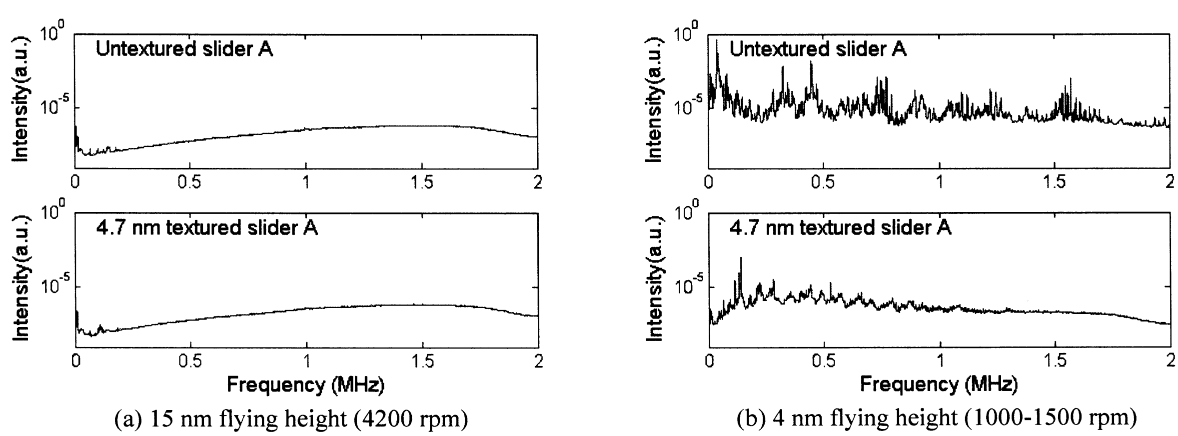

Figure 5. Out-of-plane frequency spectrum of slider A as a function of texture height.

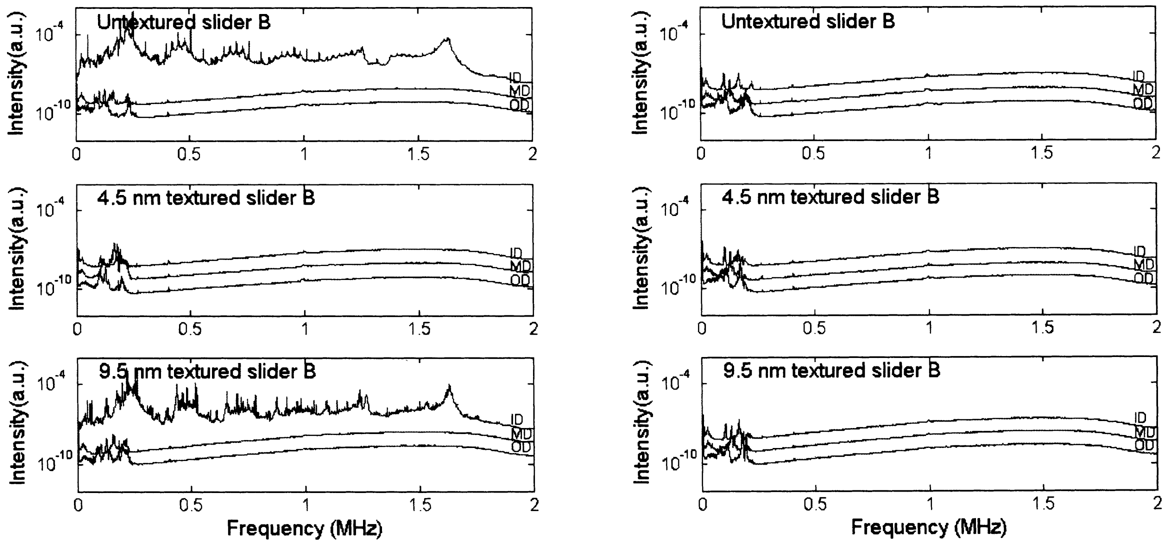

(a) 5400 rpm (b) 7200 rpm

Figure 6. Out-of-plane frequency spectrum of slider B on disk A.

Figure 8 shows the acoustic emission signal (AE) for untextured and textured sliders B with 4.5 nm and 9.5 nm texture height at the inner diameter on disk B at 7200 rpm. The amplitude of the AE signal for the 4.5 nm textured sliders is lower than that of the untextured and the 9.5 nm textured sliders.

Figure 9 shows the out-of-plane vibration spectra of slider B flying on the laser textured landing zone of disk A at 5400 and 7200 rpm, respectively. We observe slider torsion and bending modes. The intensity of the two modes is lower for the 4.5 nm textured sliders than for either the untextured or the 9.5 nm textured sliders.

3.3. Glide tests

To investigate whether the observed vibration behavior of the textured and the untextured sliders has an effect on the lubricant distribution on the disk surfaces, measurements of the lubricant thickness uniformity were performed using a Surface Reflectance Analyzer (SRA).

Figure 10 shows the SRA lubricant thickness mapping results on disks A and B after glide tests. The lighter areas correspond to regions with increased lubricant thickness, while the darker areas correspond to regions with decreased lubricant thickness. For both

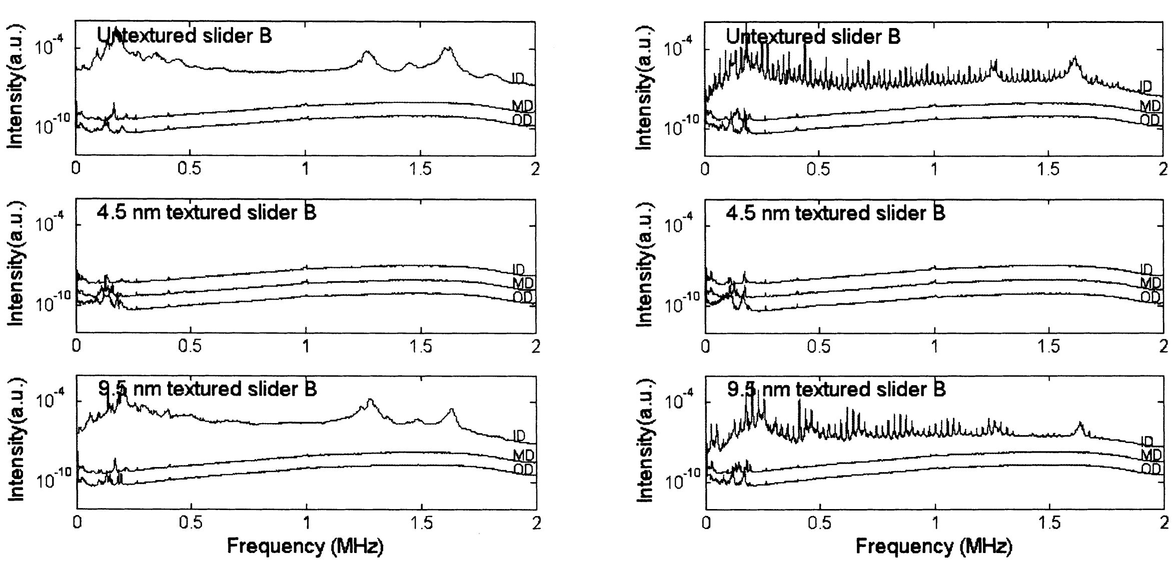

(a) 5400 rpm (b) 7200 rpm

Figure 7. Out-of-plane frequency spectrum of slider B on disk B.

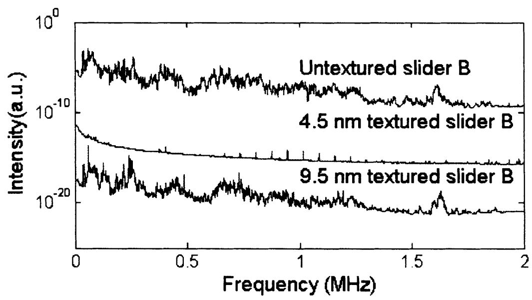

Figure 8. AE spectrum of slider B at inner diameter of disk B at 7200 rpm (flying height: 7 nm).

slider types A and B, textured sliders show less lubricant depletion than untextured sliders. For slider A, the lubricant depletion occurs mostly at the center of the "wear track", i.e., at a position corresponding to the trailing pad. For slider B three tracks are seen corresponding to the position of the trailing pad and the two side pads near the trailing edge. Lubricant thickness modulation is observed in the two side tracks for slider B. The modulation shows a frequency of around 190 kHz.

4. Discussion

Figure 4 and figure 5 show that the dynamics of slider A is not affected by surface texture at a flying height of 15 nm. We also note that contact induced slider vibrations decrease for textured slider "A". The reduction of the frictional force at the head/disk interface for textured sliders appears to be the reason for the observed reduction in the magnitude of in-plane and out-of-plane vibrations of the slider, since intermittent contacts between the slider and disk excite air-bearing modes and slider rigid body vibration modes.

For slider B, slider bending and torsion vibrations are observed only at the inner diameter (figure 6 and 7). These vibrations are stronger at 5400 rpm than at 7200 rpm. The reduced flying height caused by lower linear disk speed seems to be the reason for the observed vibrations. Furthermore, the 4.5 nm textured sliders show lower slider vibrations than the untextured sliders or the 9.5 nm textured sliders. Thus, it is apparent that surface texture reduces slider vibrations by reducing friction between slider and disk. However, since a large increase in surface texture is likely to reduce the flying height and thereby causing increased contacts between the slider and the disk, very high texture will cause additional slider vibrations. Figure 6 and 7 also show that slider vibrations on disk B are stronger than those on disk A due to the smoother surface of disk B.

Figure 9 shows that in the laser-textured landing zone, slider bending vibrations are stronger than torsion vibrations at 7200 rpm. However, bending vibrations are lower than torsion vibrations at 5400 rpm. The bending mode vibrations are excited by slider/disk contact occurring at the trailing edge of the trailing pad, while torsion mode vibrations are excited by contacts at the side pads. Thus, it is apparent that the slider flying behavior, in particular the roll and pitch stiffness, changes between 5400 and 7200 rpm. In the laser textured landing zone, contacts of the slider with the laser bumps on the disk surface occur at both 5400 and 7200 rpm, because the flying height (about 7 nm) is lower than the bump height (10 nm). At 7200 rpm, contacts between slider and laser bumps occur mostly at the trailing pad. However, at 5400 rpm, the two side pads near the trailing edge are also involved in contacts due to the reduced flying height.

The reduced slider vibration of the 4.5 nm textured sliders causes less damage on the disk surface than the

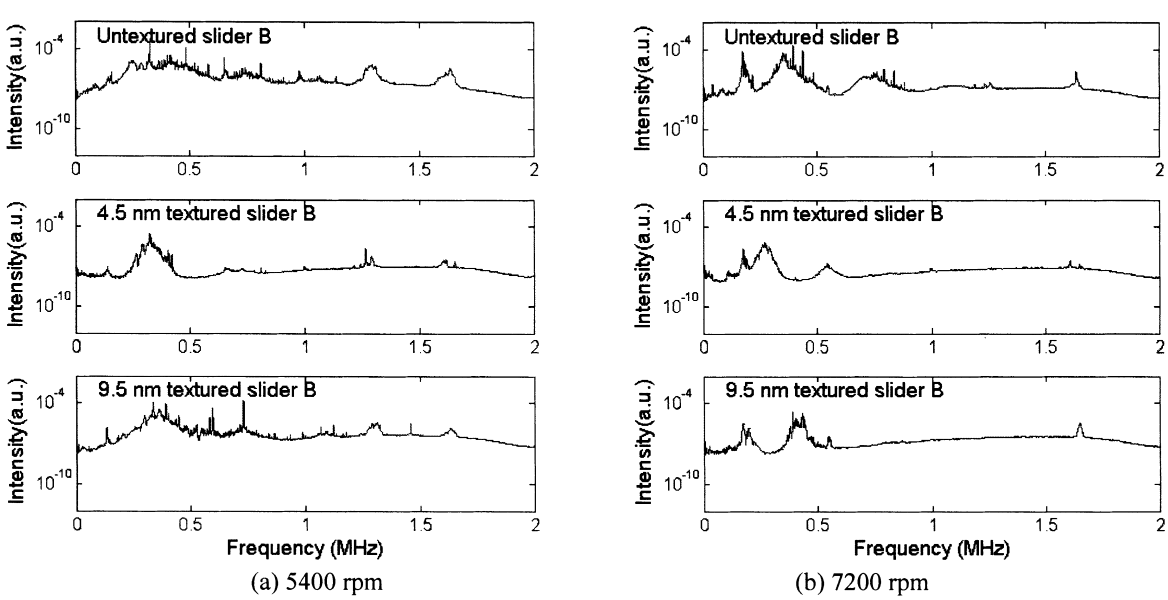

Figure 9. Out-of-plane frequency spectrum of slider B on disk A in laser textured zone.

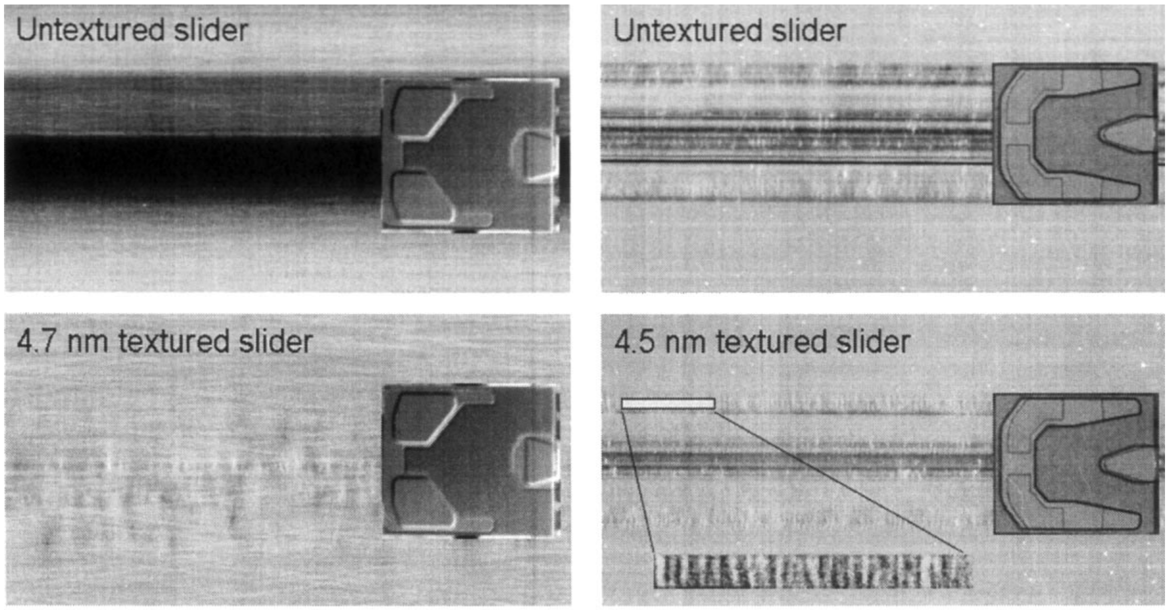

(a) Slider A/disk A
(flying height : 4 nm, 1000-1500 rpm)

(b) Slider B/disk B
(flying height : 7 nm, 7200 rpm)

Figure 10. Lubricant thickness mapping on disk surface using a surface reflectance analyzer (SRA).

untextured sliders or the 9.5 nm textured sliders. The SRA observations also show that 4.5 nm textured sliders cause less lubricant depletion than the untextured sliders (figure 10).

Ma *et al.* [18] observed lubricant thickness modulations in near contact situations between 50 and 200 kHz. Ma suggested that the roll and pitch mode vibrations of the slider is responsible for the lubricant thickness modulation. Pit *et al.* [19] observed another type of lubricant redistribution, characterized as "moguls", in the "wear track" and suggested that moguls were formed by van der Waals forces between the slider and the lubricant film. They calculated an increase in the height of the moguls with decreasing flying height.

Figure 11 shows thickness modulation and the frequency spectrum of the lubricant layer in a typical "wear track". Figure 12 compares the lubricant modulation frequencies measured using the SRA and the slider pitch mode frequencies measured using the LDV. In our results, the frequency of the lubricant thickness modulation is close to the pitch frequency of the slider. If the pitch vibration of the slider is responsible for the lubricant thickness modulation, the results indicate that the lubricant thickness modulation must be erased and reformed in each cycle.

5. Conclusions

Two types of pico-sliders were textured using ion beam etching and plasma etching. The flyability and slider dynamics of textured and untextured sliders was compared at normal and reduced disk speeds. The

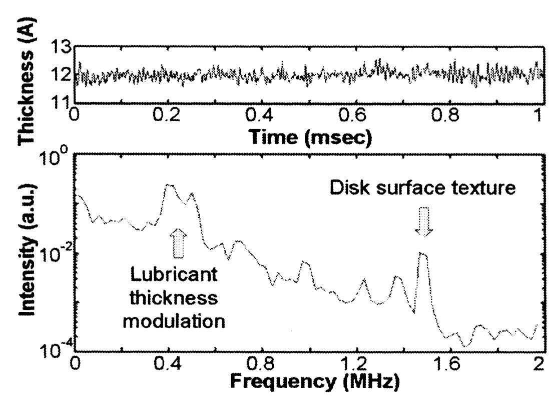

Figure 11. Lubricant thickness variation and its frequency spectrum.

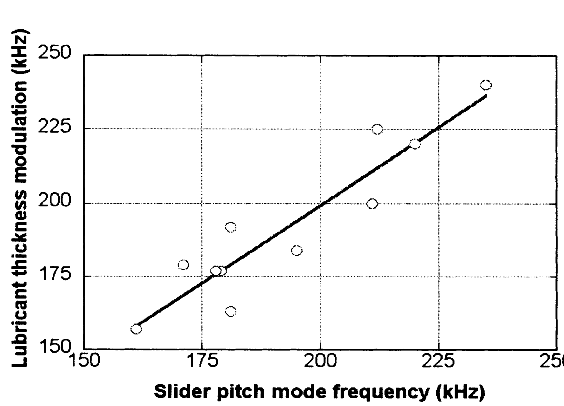

Figure 12. Lubricant modulation frequency versus pitch mode frequency.

results show that:

(1) Slider vibrations and lubricant depletion on the disk surfaces were reduced as a consequence of texturing.
(2) An optimum texture height exists which minimizes slider vibrations.
(3) Slider vibrations increase with decreasing disk surface roughness or decreasing disk speed.

6. Acknowledgments

This research was supported in part by a grant from the National Storage Industry Consortium (NSIC) and the Max Planck Stiftung in Germany.

References

[1] A.K., Menon, *ASME Proceedings of the Symposium on Interface Technology Towards 100 Gb/ in^2*, Vol. 9 (1999) p. 1.
[2] R. Ranjan, D.N. Tromel, M. Tromel, P. Golia and Y. Li, J. Appl. Phys. 69 (1991) 5745.
[3] P. Baumgart, D. Krajnovich, T. Nguyen and A.C. Tam, Data Storage, March 1996, 21–26.
[4] A. Khurshudov, B. Knigge, F.E. Talke, P. Baumgart and A. Tam, IEEE Trans. Magn. 31(6) (1997) 3190.
[5] P. Levi and F.E. Talke, IEEE Trans. Magn. 28(5) 2877.
[6] T.G. Jeong and D.B. Bogy, Tribol. Trans. ASME, 114(3) 507.
[7] Y.L. Zhu, B. Liu, W. Hua, G. Sheng and T. Yamamoto, J. Appl Phys 1 (2000) V87(N9 PT3), 6149.
[8] J. Gui, H. Tang, L.P. Wang, G.C. Rauch, Z. Boutaghou, J. Hanchi, T. Pitchford and P. Segar, J. Appl Phys. 87(9) (2000) 5383.
[9] L. Zhou, K. Kato, G. Vurens and F.E. Talke, Tribol Int. 36, 2003, 269.
[10] T. Chen, personal communication.
[11] L. Zhou, K. Kato, N. Umehara and Y. Miyake, Adv. Info. Stor. Syst. 9 (1998) 263.
[12] L. Zhou, K. Kato, N. Umehara and Y. Miyake, Tribol. Int. 33 (2000) 665.
[13] J. Hanchi, C.I. Serpe, W. Qian and Z. Boutaghou, *Proc. of Symposium on Nanotribology and Nanotechnology for 1 Tbit/in2, TRIB-Vol. 11*, 19.
[14] J. Xu, H. Tokisue, H. Tanaka and M. Matsumoto, *Proc. of 2001, STLE/ASME International Joint Tribology Conference, San Francisco, Oct. 21–24*, (2001).
[15] L. Zhou, M. Beck, H. H. Gatzen, K. Kato, G. Vurens and F. E. Talke, IEEE Trans. Magn. 38(5) (2002) 2159.
[16] L. Zhou, K. Kato, N. Umehara and Y. Miyake, Wear 243 (2000) 133.
[17] L. Zhou, N. Umehara, Y. Miyake and K. Kato, *Proc. of International Tribology Conference, Nagasaki Japan, Nov.* (2000).
[18] X. Ma, H. Tang, M. Stirniman and J. Gui, *Proc. of 2001 STLE/ ASME International Joint Tribology Conference, San Francisco, Oct. 21–24*, (2001).
[19] R. Pit, B. Marchon, S. Meeks and V. Velidandla, Tribol. Lett. 10(3) (2001) 133.